Lattice Model of Polymer Melt Intercalation in Organically-Modified Layered Silicates

Richard A. Vaia*,† and Emmanuel P. Giannelis*

Department of Materials Science and Engineering, Cornell University, Ithaca, New York 14853

Received September 22, 1995; Revised Manuscript Received September 16, 1997[⊗]

ABSTRACT: A mean-field, lattice-based model of polymer melt intercalation in organically-modified mica-type silicates (OLS) has been developed. In general, an interplay of entropic and energetic factors determines the outcome of polymer intercalation. Free energy curves and their dependence on energetic and entropic factors suggest three possible equilibrium states—immiscible, intercalated, and exfoliated—all of which have been experimentally observed. The entropic penalty of polymer confinement may be compensated for by the increased conformational freedom of the surfactant chain as the layers separate. When the total entropy change is small, small changes in the system's internal energy will determine if intercalation is thermodynamically possible. Complete layer separation, though, depends on the establishment of very favorable polymer−OLS interactions to overcome the penalty of polymer confinement. For alkylammonium-modified layered silicates, a favorable energy change is accentuated by maximizing the magnitude and number of favorable polymer−surface interactions while minimizing the magnitude and number of unfavorable apolar interactions between the polymer and the functionalizing alkyl surfactants.

1. Introduction

Materials having constituents with dimensions on the nanometer scale are currently topics of intense research. This activity is motivated, in part, by the realization that nanoscale materials often exhibit physical and chemical properties that are dramatically different from their bulk counterparts.[1−3] Recently, polymer melt intercalation has been shown to be a more efficient and environmentally-benign alternative to traditional intercalation processes for synthesis of nanophase polymer−silicate hybrids.[4−7] Traditional synthetic schemes involve intercalation of polymers either via intercalation of a suitable monomer and subsequent polymerization[8−23] or via polymer intercalation from solution.[23−27] For most technologically important polymers, these conventional approaches are limited, since neither a suitable monomer nor a compatible polymer−host solvent system is always available. Alternatively, using a variety of commercial and model polymers, polymer melt intercalation has led to a wide variety of nanophase hybrids—many of which had not been previously synthesized using the traditional intercalation approaches.

Unfortunately, many aspects of the melt intercalation process, such as the effect of silicate functionalization and intermolecular interactions on the final hybrid structure, are not well understood. Theoretical explanations of the driving forces, critical system parameters, and the potential products of the process are unavailable. Consequently, the outcome of the synthesis procedure for a specific polymer−silicate combination is not always known a *priori*.

In this paper, we develop a mean-field, lattice-based model to describe polymer melt intercalation in organically-modified mica-type layered silicates. The resulting thermodynamic model is used to discuss the contributions of various entropic and energetic factors to the free energy of the system upon hybrid formation and to identify possible equilibrium states of the hybrids. By addressing the thermodynamic aspects of the process, our aim is to establish a framework where melt intercalation may be critically explored and where guidelines for hybrid synthesis can be established. In a follow-up paper, the effects on hybrid formation of various characteristics of the silicate and polymer (e.g., intermolecular interactions, nature of silicate functionalization) will be qualified by contrasting the mean-field model with the experimental results.[28]

2. Background

Mica-type layered silicates possess the same structural characteristics as the well-known minerals talc and mica.[29,30] Their crystal structure consists of two-dimensional layers formed by fusing two silica tetrahedral sheets with an edge-shared octahedral sheet of nominally aluminum or magnesium oxide. Stacking of the layers leads to a van der Waals gap or gallery between the layers. The galleries (alternatively referred to as the interlayers) are normally occupied by cations that balance the charge deficiency that is generated by isomorphous substitution within the layers (e.g., Al for Si or Mg for Al). Commonly, hydrated alkali metal and alkali earth cations balance the layer charge, creating a hydrophilic interlayer environment.

Organically-modified layered silicates (OLS) are produced by a cation-exchange reaction between the silicate and an alkylammonium salt (surfactant molecule).[30,31] Because the negative charge originates in the silicate layer, the cationic head group of the alkylammonium molecule will preferentially reside at the layer surface and the aliphatic tail will radiate away from the surface. The interlayer structure of the aliphatic chains ranges from solid-like to liquidlike but is disordered with a density comparable to liquid alkanes at temperatures greater than ∼100 °C.[31] The presence of these aliphatic chains in the galleries renders the originally hydrophilic silicate organophilic.

Figure 1 schematically shows hybrid formation by direct polymer melt intercalation in organically-modified silicates (OLS). The synthesis involves annealing, statically or under shear, a mixture of the polymer and silicate above the softening point of the polymer.[4−7]

† Present address: Polymer Branch, Materials Directorate, Air Force Research Laboratory, Wright-Patterson AFB, OH 45433.

[⊗] Abstract published in *Advance ACS Abstracts,* November 15, 1997.

S0024-9297(95)01433-1 CCC: $14.00

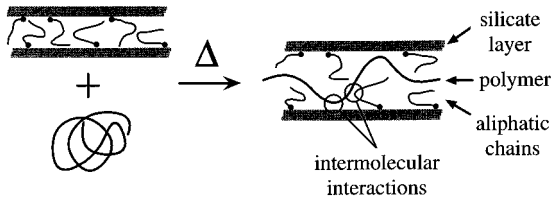

Figure 1. Schematic depicting the intercalation process between a polymer melt and an organically-modified layered silicate (OLS). The interlayer density before and after intercalation is 0.8−1.0 g/cm^3.

During the anneal, the polymer chains diffuse from the bulk polymer melt into the galleries between the silicate layers. Depending on the degree of penetration of the polymer into the OLS structure, hybrids are obtained with structures ranging from *intercalated* to *exfoliated*. Polymer penetration resulting in finite expansion of the silicate layers produces intercalated hybrids consisting of well-ordered multilayers composed of alternating polymer/silicate layers. Extensive polymer penetration resulting in disorder and eventual delamination of the silicate layers produces exfoliated hybrids consisting of individual nanometer-thick silicate layers suspended in a polymer matrix.

Hybrids have been obtained from polymers with varying degrees of polarity and crystallinity, implying that polymer melt intercalation is a general phenomenon.[4−7,28] The structure of the hybrid may be controlled by altering the length, density, and type of surfactant modifiers of the OLS, as well as the polymer.

The final polymer−OLS structure closely resembles many idealized depictions of confined polymer systems. The thermodynamics of confined polymers has been an area rich in theoretical development over the past 30 years. Numerous models, varying in complexity, have been developed to describe confined polymer melts and polymer brushes,[32−40] amphiphilic bilayers and monolayers,[41−44] and block copolymer−homopolymer blends.[45−48] Surprisingly, none of these theoretical models capture all the aspects of the intercalation process. The interlayer structure of the intercalated hybrids consists of polymer and short surfactant chains, free and tethered to the surface, respectively. Additionally, the concentration of the polymer varies from a melt outside the interlayer to a dilute solution within the interlayer. For the majority of these theoretical treatments, only one aspect of the hybrid's interlayer structure is addressed. For example, confined polymer molecules surrounded by a monomeric solvent have been discussed, but confined polymer molecules surrounded by an end-tethered, oligomeric solvent have received relatively little attention.

In general, any comprehensive thermodynamic description of polymer melt intercalation must not only consider the potential configurations of the constituents but also consider the numerous interactions between the constituents and the interdependence of the conformations of the various constituents. For the simplest case of a polymer in a solvent, a comprehensive thermodynamic description that is generally applicable to a broad range of polymer−solvent combinations is extremely complex. For more intricate systems such as polymer melt intercalation, a comprehensive description is impractical. The present model is an initial step to understanding the important factors controlling polymer intercalation. Although simplistic, the semiquantitative mean-field model elucidates the important aspects of the process and serves as a framework for interpretation of experimental results and as a starting point for future theoretical development.

3. Model

3.1. System. As an initial approach to developing a thermodynamic description of polymer melt intercalation, consider an incompressible system with a constant density of polymer and end-tethered chain segments. A single interlayer of OLS with a spacing of h_0 is embedded in a bath of polymer melt where the interlayer is completely occupied with end-tethered surfactant chains. As the interlayer spacing increases, polymer is incorporated from the surrounding melt, producing an intercalated polymer−OLS hybrid. In a mean-field context, we assume the free energy change associated with layer separation and polymer incorporation may be separated into an internal energy change associated with the establishment of new intermolecular interactions, ΔE, and an ideal combinatorial entropy change associated with configurational changes of the various constituents, ΔS. Thus, the total change in Helmholtz free energy, ΔF, accompanying layer separation from an unintercalated interlayer of gallery height h_0 to a polymer-intercalated interlayer of gallery height h is

$$\Delta F = F(h) - F(h_0) = \Delta E - T\Delta S \tag{1}$$

where T is temperature. $\Delta F < 0$ indicates layer separation is favorable, while $\Delta F > 0$ implies the initial unintercalated state is favorable.

From the schematic in Figure 1, the major factors contributing to the free energy change may be identified as the relative confinement of the polymer, the conformational changes of the tethered chains, and the establishment of new intermolecular interactions between the polymer, the tethered chains, and the silicate surface. By separating and developing expressions for ΔE and ΔS independently, we will only indirectly account for the effect of intermolecular interactions on conformational freedom of the polymer and the OLS. Though not the ideal situation, this approach has proven very successful in semiquantitatively describing many systems such as polymer solutions.[49]

Since the system is incompressible and the silicate layer area, A, is unaltered by polymer intercalation, the interlayer volume fraction, $\hat{\varphi}_i$, of the intercalated polymer ($i = 1$) and the end-tethered surfactant chains ($i = 2$) can be expressed in terms of gallery height, h, by

$$\hat{\varphi}_2 = \frac{V_{\text{aliphatic chains}}}{V_{\text{interlayer}}} = \frac{h_0 A}{hA} = \frac{h_0}{h} \tag{2a}$$

$$\hat{\varphi}_1 = 1 - \hat{\varphi}_2 = 1 - \frac{h_0}{h} \tag{2b}$$

Initially, the interlayer volume fraction of the intercalated polymer, $\hat{\varphi}_1$, equals 0 and the gallery height equals h_0. As the gallery height increases, the additional interlayer volume is occupied by the intercalating polymer. Since end-tethered surfactant chains are present on both surfaces, the tethering of the surfactant chains prevents uniform mixing when $h > 2h_\infty$ where h_∞ is the fully extended length of the tethered chains. In this case a two-phase system exists with mostly polymer present in the central region of the gallery. Therefore, the mean-field approximation is only valid for $\hat{\varphi}_1 < 1 - (h_0/2h_\infty)$, limiting the degree of layer

expansion that may be considered. However, layer expansion up to $2h_\infty$ is sufficient to include the equilibrium interlayer spacing of most intercalated hybrids and the initial stages of layer expansion of exfoliated hybrids.[7]

Employing lattice-based statistical thermodynamics, we develop in the following sections approximate analytical expressions for ΔE and ΔS that are subsequently used to discuss the most important factors contributing to hybrid formation.

3.2. Entropy Change. The change in configurational entropy during hybrid formation, ΔS, arises from changes associated with the OLS and the intercalated polymer. For the polymer, conformational changes arise from the confinement of a polymer, initially in the melt, to a polymer−surfactant solution within a slit. For the OLS, conformational changes arise from reorganization of the silicate layers and the tethered surfactant molecules as polymer intercalates. Because the silicate layers are large (lateral dimensions $\sim 1\ \mu$m) and unaltered during intercalation, their translational entropy is relatively small and will not contribute substantially to the overall entropy change of hybrid formation. Thus, in the limit of intercalated structures with finite gallery heights, the translational component of the silicate layers may be ignored. However, relative to the unintercalated state, the tethered chains gain substantial configurational freedom as the gallery height increases, irrespective of the final hybrid structure, and thus depends on the degree of layer separation.

As a first-order approximation, we assume that ΔS can be treated as the sum of (a) the entropy gain of the tethered chains in the interlayer from increasing the gallery height from h_0 to h (ΔS^{chain}) and (b) the entropy loss in confining an initially unconstrained polymer to a gallery of height h ($\Delta S^{\text{polymer}}$).

$$\Delta S \approx \Delta S^{\text{chain}} + \Delta S^{\text{polymer}} \tag{3}$$

The implications of treating the entropic changes of the silicate and polymer in this manner warrants further comment. In the confined environment of the interlayer, the most probable segment density distribution of the tethered chains dictates the available volume for the polymer and vice versa. Subdividing the entropy of the system assumes that the configurations of the tethered chains and polymer are independent, consistent with the mean-field treatment. Realistically, this is not the case in the confined interlayer environment. However, previous work based on mean-field chain statistics indicates that this crude approximation leads to surprising realistic results, especially in identifying the major factors contributing to the chain behavior.[32,49] Since our objective is to describe the system semiquantitatively and no previous theoretical or experimental information is available to substantiate a more complex self-consistent treatment, the simplifications implicit in this approach are acceptable as an initial approach to understanding the entropic factors contributing to polymer melt intercalation.

3.2.1. Organically-Modified Layered Silicate. A modification of the Flory−Huggins lattice theory of polymer−monomer mixtures may be employed to determine ΔS^{chain}. To approximate the silicate interlayer, the modified treatment must account for (1) the restricted freedom of the tethered chains arising from the ionic interactions between the head group and the silicate layer and (2) the influence of the silicate surface on the conformational freedom of the tethered chains.

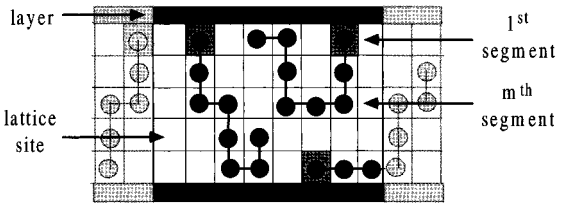

Figure 2. Two-dimensional schematic of a section of the modified lattice used to determine the interlayer entropy. The lattice has n_0 interlayer sites occupied by $n_2 - i$ tethered chains with m_2 segments per chain.

Consider a lattice of n_0 sites arranged between two impenetrable surfaces, Figure 2. The surfaces are separated by h/a_2 lattice sites such that $n_0 = h/a_2A'$. a_2 is the segment length of the tethered chain and $A' = A/a_2^2$ is the number of lattice sites in contact with one of the surfaces. The interlayer is uniformly occupied by n_2 tethered chains composed of m_2 segments. From classical mean-field lattice statistics,[49] the configurational entropy of chains on a lattice can be approximated if the total number of conformations, η_{i+1}, available to the $(i+1)$th chain can be expressed. Following the development of Barrer *et al.*,[50] if i tethered chains are already inserted into the lattice, $n_0 - m_2 i$ cells will remain unoccupied and η_{i+1} may be expressed as

$$\eta_{i+1} = (n_2 - i)(z-1)^{m_2-1}\left(\frac{n_0 - m_2 i}{n_0}\right)^{m_2-1} c^{(m_2-1)\chi_s} \tag{4}$$

To account for the restricted freedom of the chains end-tethered to the surface, the first segment of the chain is restricted to n_2 sites near the interlayer surface instead of being free to occupy all n_0 sites.[50] The probability that a site adjacent to a proceeding segment is unoccupied depends on the fraction of unoccupied sites, $(n_0 - m_2 i)/n_0$, the coordination number of the lattice, z, and a statistical surface factor, c, that accounts for the inaccessibility of sites on the far side of the surface ($c = 0.75$ for $z = 4$, $c \to 0.5$ for $z \to \infty$, where z is the coordination number of the lattice).[50] The statistical surface factor is present only for the fraction of interlayer sites near the surface that are occupied by the tethered chain, χ_s. Here $\chi_s(h_0) \equiv \chi_{s0}$ and $\chi_{s0} > \chi_s(h > h_0)$.

The total number of ways, Ω, that n_2 sets of m_2 adjacent sites can be arranged on the lattice is then

$$\Omega = \frac{1}{n_2!}\prod_{i=1}^{n_2}\eta_i = \frac{1}{n_2!}\prod_{i=1}^{n_2}\frac{(n_0 - m_2 i)!}{(n_0 - m_2(i+1))!} \times \left(\frac{z-1}{n_0}\right)^{m_2-1}\frac{n_2 - i}{n_0 - mi}c^{(m_2-1)\chi_s} \tag{5a}$$

$$= \underbrace{\frac{n_0!}{(n_0 - m_2 n_2)!\,n_2!}\left(\frac{z-1}{n_0}\right)^{(m_2-1)n_2}}_{\text{ideal combinatorial mixing}} \times \underbrace{\frac{n_2!\left(\frac{n_0}{m_2} - n_2\right)!}{\frac{n_0}{m_2}!}\left(\frac{n_0}{(n_0 - m_2 n_2)m_2^{n_2}}\right)}_{\text{restricted location of first chain segment}} \underbrace{c^{(m_2-1)\chi_s n_2}}_{\text{surface}} \tag{5b}$$

and the configurational entropy of the system is given by $S^{chain} = k_B \ln \Omega$. Equation 5b may be separated into three components. The initial term is the traditional expression obtained by Flory[49] for placing chain molecules on an unconstrained lattice and leads to an expression for the ideal translational entropy of the system. The second term arises from the restraints imposed on the location of the first chain segment that is end-tethered. The third term accounts for the effect of the silicate surface on the conformations of the tethered chains by reducing the possible number of adjoining sites by the fraction of lattice sites near the silicate surface.

Using Sterling's approximation for the factorials in eq 5b and normalizing to interlayer volume,[49,51] the entropy change of the interlayer may be expressed. The entropy change per interlayer volume of the tethered chains, Δs_V^{chain} with layer separation from h_0 to h is given by

$$\frac{\Delta s_V^{chain}}{N_A k_B} = \frac{1}{N_A k_B}(s_V^{chain}(h) - s_V^{chain}(h_0)) = \frac{-1}{m_1 \nu_1}\hat{\varphi}_1 \ln(\hat{\varphi}_1) + \frac{1}{\nu_2}\hat{\varphi}_2 \ln(c)(\chi_S - \chi_{S0}) \quad (6)$$

where ν_i, m_i, and $\hat{\varphi}_i$ are the molar volume per segment, the number of segments per chain, and the interlayer volume fraction, respectively. N_A and k_B are Avogadro's number and Boltzmann's constant, respectively. Additionally, the approximations that $(m_2 - 1) \approx m_2$ and $(1 - 1/m_2) \approx 1$ are made.

Equation 6 indicates that the end-tethering of chains effectively removes their translational contribution to the entropy. The additional interlayer volume associated with layer separation increases the entropy of the tethered chains by effectively decreasing the influence of the surface on their conformations by $(\chi_S - \chi_{S0})$. For polymer melt intercalation, the medium surrounding the tethered chains consists of polymer whose length, m_1, is large, and thus the translational component associated with the polymer (first term in eq 6) will be small. The entropy change of the interlayer with increasing interlayer spacing is dominated by the effect of the surface on the conformational freedom of the tethered chains and

$$\Delta s_V^{chain}/N_A k_B \approx \frac{1}{\nu_2}\hat{\varphi}_2 \ln(c)(\chi_S(h) - \chi_{S0}) \quad (7)$$

Therefore, as layer separation increases, the entropy change is proportional to the difference in the fraction of interlayer sites near the retreating surface, $\chi_S(h) - \chi_{S0}$. Recall that χ_S is strictly defined as the fraction of interlayer sites next to the surface that are *accessible* by the end-tethered chains. In other words, $\chi_S(h) - \chi_{S0}$ represents the influence of the opposing surface on the potential chain conformations. The fraction of interlayer sites near a surface is a_2/h; however, sites that are at a distance greater than h_∞ from the tethering point are inaccessible to the end-tethered chain and do not influence the potential chain conformations. As the gallery height approaches h_∞, the fraction of sites near the surface that influence the potential location of tethered chain segments on the lattice approaches zero. The functional dependence of $\chi_S(h)$ may be approximated in a variety of ways.[52] Assuming the segment density distribution of an unconstrained end-tethered chain can be crudely expressed by Gaussian (random flight) statistics, the density of tethered chain segments perpendicular to the surface decays as $\cos^2(\pi h/2h_\infty)$ with distance, h, from the tethering surface.[34,53] Therefore, with regard to the limit at h_∞, $\chi_S(h)$ can be constructed as

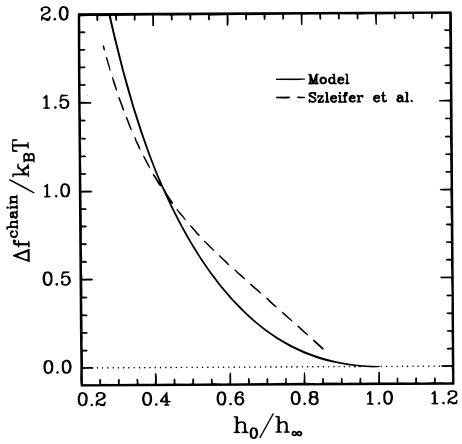

Figure 3. Ideal free energy change per 12-carbon end-tethered aliphatic chain upon complete separation of the confining layers for a series of OLS's with different tethering densities. Higher tethering density corresponds to greater initial gallery heights and h_0/h_∞ approaching unity. The lattice model (solid curve) assumes the volume and extended length of the tethered alkyl chain are 12 (0.027 nm^3) and 12 (0.127 nm), respectively. Szleifer *et al.*'s values[44] (dashed curve) are calculated from the free energy difference per chain between a compacted monolayer and a "free" monolayer with an area per chain equal to the volume per chain divided by the layer height. We assume the free monolayer is equivalent to an interlayer with $h > h_\infty$.

$$\chi_S(h) = \frac{a_2}{h}\cos^2\left(\frac{\pi}{2}\frac{h}{h_\infty}\right) \qquad h < h_\infty \quad (8)$$

where $\chi_S(h \geq h_\infty) = 0$. The advantage of eq 8 is that $\chi_S(h)$ smoothly and continuously approaches zero as $h \rightarrow h_\infty$.[52]

The validity of eq 8 may be examined by comparing it to results from more sophisticated theories such as those of Szleifer *et al.*[43,44] Figure 3 shows the free energy change per 12-carbon end-tethered aliphatic chain upon complete separation of the confining layers for a series of OLS's with different tethering densities. Higher tethering density corresponds to greater initial gallery heights and h_0/h_∞ approaching unity. The dashed curve was determined by Szleifer *et al.*[43,44] for the case when the internal energy of the system is constant ($\Delta f^{chain}/k_BT = -\Delta s^{chain}$). The solid line is determined using the lattice model (eqs 7 and 8) for the same situation where $\Delta f^{chain}/k_BT = -\ln(c)(h_\infty/h_0 \cos^2(\pi h_0/2h_\infty))$. We assume the volume and extended length of the tethered alkyl chain is 12(0.027 nm^3) and 12(0.127 nm), respectively. Note that Δf^{chain} represents the free energy gain per chain (not that per interlayer volume). When the interlayer spacing increases from $h = h_0$ to $h > h_\infty$, then $\chi_S(h) - \chi_{S0} = -\chi_{S0}$.

In general, the results from the lattice model exhibit a similar trend to that determined from the more sophisticated approach of Szleifer *et al.*[43,44] For $0.5 < h_0/h_\infty < 1$, the lattice model underestimates the entropy gain associated with layer separation. This arises from our description of the segment density profile across the interlayer (eq 8) and is in accordance with predicted segment density profiles for tethered oligomeric chains whose profiles decrease less rapidly away from the

surface than predicted by random flight statistics.[41−44] Although the agreement is not perfect, the advantage of eqs 7 and 8 is that the effect of constraining the tethered chains on the entropy of the system can be approximated analytically. At this time, further improvement to eq 8 is unjustified given the various approximations in eq 7.

3.2.2. Confined Polymer. To complete the expression for ΔS, the entropy change associated with the intercalated polymer must be expressed in a manner complimentary to ΔS^{chain}. In a mean-field context, the total entropy change associated with polymer confinement may be expressed as the product of the interlayer volume fraction of polymer and the entropy loss of a polymer chain confined to a slit height equal to the gallery height of the hybrid. Numerous mean-field descriptions of polymers confined between two flat surfaces have been proposed.[32,34,36−38,40] Of these, the Dolan and Edward's treatment of confined random-flight polymer chains are closest to our modified Flory approach for the silicate interlayer.[34]

Following Dolan and Edward's methodology to calculate the entropy loss of a confined random-flight polymer chain with excluded volume, the entropy loss per interlayer volume of the intercalated polymer, $\Delta s_V^{\text{polymer}}$, is[34]

$$\Delta s_V^{\text{polymer}}/N_A k_B = -\frac{\hat{\varphi}_1}{\nu_1}\frac{\pi^2}{6}\left(\frac{a_1}{h}\right)^2 - \frac{\hat{\varphi}_1}{\nu_1}\sqrt{\frac{3}{m_1}}u\frac{a_1}{h} \quad (9)$$

where v_1, a_l, and m_1 are the molar volume per segment, the segment length, and degree of polymerization of the polymer, respectively. u is Dolan and Edward's dimensionless excluded volume parameter. By defining the volume of a lattice site as the volume of a surfactant unit, a_l is related to the radius of gyration of the polymer R_g, by $a_1^2 = 6R_g^2\nu_2/\nu_1 m_1$ or alternatively, by $a_1^2 = a_p^2\nu_2/\nu_1$, where a_p is the statistical segment length of the polymer.

The first term in eq 9 describes the configurational entropy loss per interlayer volume of a confined, ideal random-flight polymer and agrees with scaling arguments developed by de Gennes.[32] Ideal random-flight statistics, though, do not account for the physical volume or the connectivity of the polymer and result in an underestimation of the total entropy change of the intercalated polymer associated with the neglect of the self-avoiding nature of a real polymer chain. Scaling arguments introduced by de Gennes and others for a self-avoiding polymer in 3-dimensions indicate that $(a_1/h)^x$ should scale as $x = 5/3$ and not as $x = 2$.[32] However, these scaling relationships are not useful in our development because the coefficients have yet to be determined and thus the absolute magnitude of various entropic terms cannot be determined. Furthermore, recent work has shown that the scaling relationship is dimensionally dependent and thus changes as the slit height approaches the size of a repeat unit.[54]

To account for the impenetrability of polymer segments and better approximate the confirmational statistics of a real polymer, the effect of excluded volume on the conformation of a confined random-flight chain was included. The excluded volume describes the influence of the interlayer environment on the polymer conformation. Assuming there is minimal interpenetration of polymer chains in the interlayer, $u \approx 3(\alpha^5 - \alpha^3)$, where α *is* the chain expansivity as defined by Flory.[49] The molecular weight dependence in the second term of eq 9 is related to the molecular weight dependence of the Flory excluded volume, v, by $v/v_1 = u/Km_1^{1/2}$ where K is a numerical constant.[34,49] Recall that the concentration of polymer segments changes as the layers separate and that the entropy change of the confined polymer is determined with respect to the polymer melt. Thus, α represents the expansion of the chain in the interlayer environment with respect to the melt and will depend on gallery height in an unknown manner, approaching zero as the concentration approaches that of the melt. Since the mean-field approximation is only valid for $h \leq 2h_\infty$, we assume α is constant, independent of h and specific for a given polymer−OLS system.

3.3. Internal Energy Chance. To complete the thermodynamic description of polymer melt intercalation, the internal energy associated with intermolecular interactions must also be included. As shown in Figure 1, the prominent interactions will arise between the three components of the system—the silicate surface, s, the tethered surfactant chains, a, and the polymer, p.[55]

Flory[49] showed that by assuming the constituents of a system interact in a mean-field, pairwise manner, the total change in internal energy is the sum of the energy change associated with each pairwise interaction. The specific distribution of the constituents within the system is less important; only the interaction energy per contact and the number of contacts per unit need to be determined. Traditionally, for lattice-based models, the number of contacts is defined by the symmetry and coordination number of the lattice. As the coordination number of the lattice approaches infinity, the number of contacts approaches the contact area. Here, the energy per contact may be equally expressed as an energy per lattice site. Using the lattice to approximate the total contact area, this alternative definition is advantageous because the pairwise interaction energy per area is lattice-independent and may be further interpreted as a cohesive or interfacial energy per area for which values are available in the literature. For polymer melt intercalation, using interfacial energies is especially advantageous because of the polar nature of the silicate surface and the presence of the alkylammonium cations. The associative interactions resulting from these polar constituents may be described using expressions for interfacial energies, such as the one developed by van Oss and co-workers.[56]

Using the area approach, the internal energy change of the system upon polymer intercalation, ΔE, is expressed as

$$\Delta E = A_{sp}^f\epsilon_{sp} + A_{ap}^f\epsilon_{ap} + (A_{sa}^f - A_{sa}^i)\epsilon_{sa} \quad (10)$$

where A_{jk}^i and A_{jk}^f are the total area of contact between the components for the initial unintercalated system and the final hybrid, respectively. ϵ_{jk} is the pairwise interaction energy per area of these contacts relative to the initial j−j and k−k interactions. Large positive values of ϵ_{jk} indicate unfavorable interactions, while negative values of ϵ_{jk} indicate favorable interactions. Equation 10 may be further simplified by assuming, as we did previously for the entropy of the tethered surfactant chains, that all the lattice sites are initially occupied by tethered chain segments. Therefore, in the incompressible limit, the final area of polymer−surface contacts established equals the difference between the initial and final area of surfactant−surface contacts, such that $A_{sp}^f = A_{sa}^f - A_{sa}^i$.

To determine the fraction of interaction area between components, Konigsveld and coworker's site fraction approach[57,58] is modified by approximating the interaction area per segment, α_j, of the j-th molecular species as the circumferential area of a cylinder with height and volume equal to that of the j-th segment. Therefore, the internal energy per interlayer volume associated with intercalation, Δe_v, is

$$\Delta e_V = \hat{\varphi}_1 \hat{\varphi}_2 \frac{b}{Q} \tag{11}$$

where

$$b = \left(\frac{2}{h_0} \epsilon_{sp,sa} + \frac{2}{r_2} \epsilon_{ap} \right) \tag{12}$$

and

$$Q = 1 - \hat{\varphi}_2 \left(1 - \frac{r_1}{r_2} - \frac{r_1}{h_0} \right) \tag{13}$$

b/Q is the effective interaction energy per interlayer volume[59] and r_i is the radius of the interaction surface, approximated as a cylinder, such that $r_i = (\nu_i / N_A)(2/\alpha_i)$ or likewise $r_i^2 = (\nu_i / N_A)(1/a_i \pi)$. Recall that the change in interactions at the interlayer surface is expressed by $\epsilon_{sp,sa} = \epsilon_{sp} - \epsilon_{sa}$.[55] ϵ_{jk} is the pairwise j−k interaction energy per area of the j−k contacts relative to the initial j−j and k−k interactions.

4. Discussion

The total free energy change associated with layer separation and polymer intercalation and its entropy and energy components may be expressed as a function of gallery height by combining eqs 1−3, 7−9, and 11−13. These expressions are based upon two critical assumptions concerning the structure of the tethered surfactant chains and the intercalated polymer: (i) disordered interlayer structure and (ii) constant segment density.

Mean-field approximations are most applicable for a random, disordered arrangement of constituents. Consequently, the model inherently assumes the interlayer structure of the OLS before and after polymer intercalation is disordered and liquid-like. Using Fourier transform infrared spectroscopy and X-ray diffraction, we have recently shown this to be the case for the unintercalated OLS at processing temperatures generally used for melt intercalation.[31] Additionally, using the same techniques, in-situ monitoring of the interlayer structure during polystyrene intercalation in an OLS indicates that the degree of disorder of the interlayer environment is the same or increases slightly as the polymer intercalates.[7]

A constant interlayer density is necessitated because we assume incompressibility to derive the internal energy and entropy expressions. Using X-ray diffraction measurements of the gallery heights of the unintercalated OLS and of the final hybrid, the interlayer density, ρ, can be approximated before and after melt intercalation. To a first approximation, the relationship between the initial gallery height and the interlayer density, ρ, may be expressed linearly as $h_0 = FW/\rho\sigma N_A$, where FW is the formula weight of the surfactant chain and σ is the area per tethered chain (determined from the silicate's exchange capacity). From the experimental gallery heights for unintercalated alkylammonium-modified fluorohectorites,[31] the initial interlayer density is approximately 0.9 ± 0.1 g/cm^3,[7] similar to the density of liquid alkanes. The interlayer density after intercalation may also be approximated in a similar fashion from the final gallery height, the molar volume of a polymer segment, and the weight fraction of polymer necessary to fully intercalate the OLS. Again, using experimental gallery heights for polystyrene melt intercalated alkylammonium-modified fluorohectorites,[7,28] we find that the final interlayer densities are within 10% of the initial interlayer densities.[7] Thus, to a first approximation, the interlayer density is invariant throughout the polymer intercalation process.

Table 1. Parameters for a Silicate Functionalized with Octadecylammonium Groups and an Arbitrary Polymer

initial gallery height	h_0	1.30 nm
tethered chain		
segment length	a_2	0.25 nm
molar vol	v_2	33 cm^3
no. of segments[a]	m_2	9.5
polymer		
statistical segment length	a_p	$2.5a_2$
molar vol	v_1	$3v_2$
excluded vol param	$u/\sqrt{m_1}$	0.8

[a] The length of the ammonium group is approximated as half of the length of a C_2H_4 unit such that $m_2 = n'/2 + 0.5$ where n' is the number of carbon atoms in the alkyl chain and $h_\infty = a_2 m_2$.[61]

Since both critical assumptions about the microscopic structure of the interlayer have an experimental basis, the following sections will use the developed expressions to discuss the important entropic and energetic factors that affect polymer intercalation and identify possible equilibrium states of the hybrids.

4.1. Entropic Factors. Upon initial examination of the melt intercalation process, the entropy decrease associated with polymer confinement between the silicate layers might be expected to be large enough to prohibit hybrid formation. During polymer intercalation from solution, the entropy loss of the intercalated polymer is compensated for by an entropy gain associated with the desorption of a relatively large number of previously absorbed solvent molecules.[60] These molecules are displaced from the interlayer to accommodate the incoming polymer chains. Since the number of alkylammonium cations in the OLS is fixed by the necessary charge balance with the silicate layer, a polymer intercalating from the melt cannot displace any interlayer species that would subsequently gain translational freedom. In the absence of strong interactions between the polymer and the silicate surface, the question arises as to what compensates the system for polymer confinement.

Although the tethered chains do not gain translational freedom, they do gain configurational freedom as the gallery height increases. This increased configurational entropy of the tethered chains may compensate the entropy loss associated with polymer confinement. Consider an example of an arbitrary polymer and a silicate functionalized with octadecylammonium groups, Table 1.[61] Using eqs 2, 3, and 7−9, $h\Delta s_V^{polymer}$, $h\Delta s_V^{chain}$, and $h\Delta s_V$ can be calculated as a function of gallery height up to $2h_\infty - h_0$ (Figure 4). Note that the entropy density is an extensive quantity because the volume of the system varies linearly with interlayer spacing. In contrast, the product of the entropy density in the interlayer and the gallery height is an intensive quantity and independent of system size.

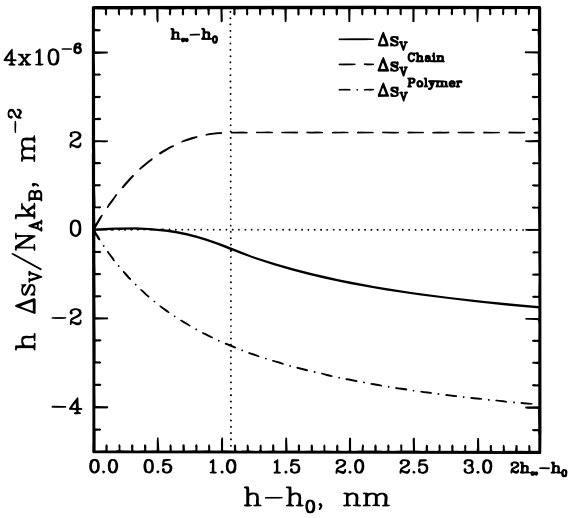

Figure 4. $h\Delta s_V^{polymer}$, $h\Delta s_V^{chain}$, and $h\Delta s_V$ as a function of the change in gallery height for an arbitrary polymer and a silicate functionalized with octadecylammonium groups (Table 1). $h_\infty - h_0$ is the change in gallery height for a fully-extended octadecyl chain.[52]

The entropy change associated with the tethered chains, $h\Delta s_V^{chain}$ (dashed line), increases until the layer separation is equal to the fully-extended length of the tethered chains, h_∞. Layer separation greater than h_∞ does not result in additional configurational freedom because the opposite surface no longer influences chain conformations. Thus, $h\Delta s_V^{chain}$ is invariant for $h > h_\infty$.

The entropy change associated with the polymer, $h\Delta s_V^{polymer}$ (dash-dot line), is small at gallery heights near h_0 since the volume fraction of polymer in the interlayer is small. As h increases, more polymer is confined and the total penalty for polymer confinement per unit silicate area increases. The magnitude of entropy loss is related to the extent of chain expansion in the interlayer. Here, $u/m^{1/2} = 0.8$, corresponding to $\alpha \approx 1.5$ for an average molecular weight polymer ($m_1 = 300$) and implying the interlayer environment is favoring athermal conditions. The excluded volume term introduces a weak molecular weight dependence, indicating that intercalation is *thermodynamically* favored for higher molecular weight polymers. However, *kinetically*, higher molecular weight chains will take longer to intercalate, potentially making this dependence difficult to observe.

The overall entropy change per area of the system, $h\Delta s_V$, is the sum of $h\Delta s_V^{polymer}$ and $h\Delta s_V^{chain}$ (Figure 4). $h\Delta s_V$ (solid line) may be qualitatively separated into two regions. For gallery heights less than a critical height, h_c, the overall entropy change is near zero. Here, the penalty for polymer confinement is compensated by entropy gains associated with layer separation ($|h\Delta s_V^{chain}| \sim |h\Delta s_V^{polymer}|$). Conversely, for $h > h_c$, the overall entropy change decreases and hybrid formation is entropically unfavorable.[52]

For the situation considered in Table 1, if $u/m^{1/2} = 0$, corresponding to Θ-conditions,[34,49] $|h\Delta s_V^{chain}| > |h\Delta s_V^{polymer}|$ implying spontaneous intercalation is possible. However, this situation is not consistent with experimental results for polymer−OLS systems in which $\Delta e_V \sim 0$ and polymer melt intercalation is not observed at least statically.[7,28] Nonetheless, the entropy loss of the polymer is in general the same magnitude as the entropy gain of the tethered chains and for systems with $\Delta e_V \sim 0$ the free energy change is also near zero. In these cases the model is rather limited in describing the outcome of intercalation due to the several assumptions and approximations used.

Thus, for successful hybrid formation, it is critical to have an initial interlayer structure that results in a maximum increase in the conformational entropy of the tethered chains to compensate the penalty of polymer confinement. We will specifically address what this optimum structure is in the followup paper.[28] Additionally, since the conformational entropy of the tethered chains only increases up to h_∞, complete layer separation depends on the establishment of very favorable interactions to overcome the penalty of polymer confinement at $h > h_\infty$.

Even though the mean-field model is limited to $h \leq 2h_\infty$, we can at least qualitatively discuss the behavior of the system at greater gallery heights. At very large layer spacings ($h >> 2h_\infty$), the entropy change per interlayer area approaches a finite limit because the configurational effects associated with the presence of the silicate surface will always contribute to $h\Delta s_V$. However, the volume fraction of the system near the silicate surfaces becomes increasingly small with increasing gallery height and the contribution of the tethered chains to the total entropy change is minimal. Additionally, when h is greater than R_0, the radius of gyration of the polymer, the penalty of polymer confinement approaches zero. Therefore, for layer separations associated with exfoliated hybrids, a complementary model considering the mixing in the bulk of n_2 silicate layers and n_1 polymer chains is a more appropriate starting point to discuss the thermodynamic stability of these hybrids. For the bulk system, the total entropy change per volume will depend on constituent mixing and will be near zero. If the functionalized silicate layers are treated as a macromolecule, the stability of these hybrids may be likened to the phase behavior of polymer blends, where small changes in the interactions between the two macromolecules drastically impact their phase behavior.[62] Even if these exfoliated hybrids are thermodynamically stable, large energy barriers associated with silicate layer separation must be overcome for melt-processing to be successful.

4.2. Energetic Factors. The total energy change of the system depends on the volume fraction of polymer in the interlayer and the effective interaction parameter, b/Q (eq 11). The magnitude and sign of b is related to the various pairwise interactions between the constituents and structural aspects of the interlayer such as packing density, accessibility of interactions sites at the interlayer surface, and size of the tethered-chain segments. Since in most conventional organosilicates the tethered surfactant chains are apolar, dispersion forces will dominate polymer−surfactant interactions, ϵ_{ap}. Therefore, the change in the interaction energy, relative to the initial surfactant−surfactant and polymer−polymer contacts, will be positive and unfavorable. On the other hand, the silicate surface is polar. Thus, polymer−surface interactions established during intercalation may be more favorable than the initial surfactant−surface contacts, resulting in the possibility of $\epsilon_{sp,sa} < 0$. Consequently, a favorable energy decrease is associated with the establishment of many favorable polar polymer−surface interactions. Since the total entropy change for intercalated hybrids is small, these interactions are expected to provide the driving force for polymer intercalation.

The interlayer concentration of the different types of interacting jk pairs, however, determines their overall effect on $h\Delta e_V$. Since the majority of the interaction area is in the central portion of the interlayer, changes in interlayer interactions, ϵ_{ap}, will have a greater effect on Δe_V than changes in the relative surface interactions, $\epsilon_{sp,sa}$. To quantify the relative effect of these interactions, we define the critical interlayer structure parameter, ξ_c, as the ratio of the prefactors of the interaction parameters, $\xi_c = h_0/r_2$ (eq 12). The prefactors express the dependence of the total energy change on the structure of the interlayer. When $\epsilon_{sp,sa}$ and ϵ_{ap} are of opposite sign and $|\epsilon_{sp,sa}/\epsilon_{ap}| = \xi_c$, the total energy change is zero. For the parameters (Table 1) used in Figure 4, $\xi_c = 5$. Therefore, to compensate for unfavorable polymer−surfactant interlayer interactions, the change in surface interactions associated with replacement of surfactant−surface interactions with polymer−surface interactions must be 5 times more favorable.

When possible polymer−OLS systems are selected, these energetic considerations imply that not only favorable polymer−surface interactions must be maximized but also that unfavorable apolar interactions between the polymer and the tethered chains must be minimized. The number of surface interactions may be maximized by choosing an interlayer structure for the OLS that minimizes ξ_c and maximizes the potential number of surface sites. This may be achieved by controlling the density or type of interlayer organic cations. There are no limitations to using only alkylammonium-modified layered silicates for polymer melt intercalation.[5,7] For example, the polymer-tethered chain interactions may be minimized by selecting organic modifiers that behave as a Θ-solvent for the polymer. On the other hand, the energetic contributions may also be maximized by incorporating certain moieties into the polymer structure that interact very favorably with the interlayer. The increased interaction between the polymer and OLS, though, may decrease the kinetics of intercalation by decreasing the diffusivity and increasing the monomeric friction coefficient of the polymer in the interlayer.

4.3. Equilibrium Phases. Thermodynamically stable equilibrium states of the hybrid will be determined by an interplay of the various entropic and energetic factors. To demonstrate the general forms of the free energy curves, consider the system used in the previous examples (Table 1). Figure 5 shows $h\Delta f_V$ at 423 K for various $\epsilon_{sp,sa}$. For simplicity, we assume $\epsilon_{ap} = 0$. This situation would describe melt intercalation of a series of polyethylene-based polymers—$\epsilon_{sp,sa} = 0$ for pure polyethylene and $\epsilon_{sp,sa} < 0$ for polyethylene copolymers in which a small fraction of ethylene units are replaced with moieties exhibiting more favorable interactions with the silicate.

The free energy curves may be grouped into three types. Type I curves are positive at all gallery heights. Polymer intercalation is unfavorable, and the polymer and OLS are immiscible. In this case, the polymer−surface interactions are similar to the surfactant−surface interactions, resulting in no net driving force for polymer intercalation.

Type II curves display a minimum at a discrete gallery height. This class can be further subdivided. For type IIa curves, only one minimum exists and polymer intercalation is favorable up to a finite layer separation, indicating that intercalated polymer−OLS states are favorable. Since the total entropy change may be small for a range of $h < h_\infty$, only a small favorable increase in the surface interactions is necessary to reduce the free energy and form a minimum. For type IIb curves, more than one free energy minimum exists and a transition from the local minimum at $h < h_\infty$ to the global minimum at $h > h_\infty$ may require external energy inputs, such as special processing considerations or an exothermic chemical reaction. Type IIb systems will exhibit ill-defined intercalated structures or intermediate intercalated structures before complete layered exfoliation.[6,7,28]

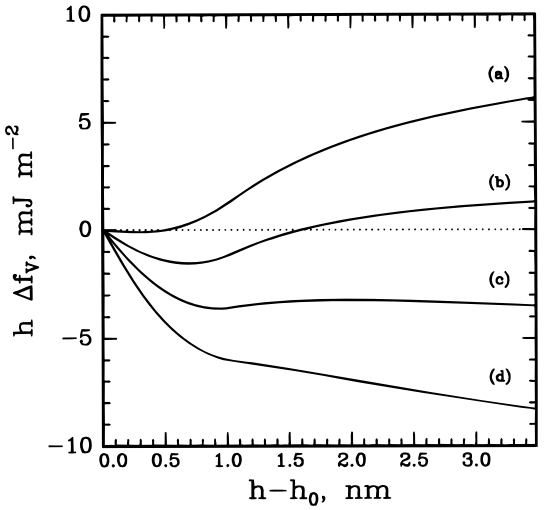

Figure 5. $h\Delta f_V$ for the system outlined in Table 1 and various $\epsilon_{sp,sa}$ with $\epsilon_{ap} = 0$. Free energy curves (a)−(d) correspond to $\epsilon_{sp,sa} = 0$, −4, −8, and −12 mJ/m^2 and, as discussed in the text, type I, IIa, IIb, and III free energy curves, respectively.

For type III curves, the free energy minimum at $h < h_\infty$ becomes less defined and $h\Delta f_V$ continually decreases as the gallery height increases. Polymer intercalation and complete layer separation is favorable. This indicates complete polymer−silicate layer miscibility, leading to an exfoliated state. Because the penalty of polymer confinement dominates at $h > h_\infty$, exfoliated structures require strong energetic interactions to overcome the unfavorable entropy changes.

The effect of temperature on the shape of the free energy curves will depend on the assumed temperature dependence of the interaction parameters and chain expansivity and thus the specific polymer−OLS system under consideration. For temperatures far from an effective interlayer Θ point, the temperature dependence of these parameters will at most be linear, and thus for conventional processing ranges temperature is not expected to drastically affect the thermodynamic state. However, the processing temperature will affect the kinetics of hybrid formation.[6] For example, the rate of hybrid formation will depend on polymer mobility and thus on the difference between the processing temperature and the glass transition temperature of the polymer.

In general, the trends discussed in Figure 5 agree well with experimental results. Immiscible, intercalated, and exfoliated structures have been experimentally obtained.[47,28,63] Intercalated hybrids are obtained in systems with somewhat weak polymer−surface interactions.[7,28,52] Discrete intercalated states are rarely observed in systems that yield exfoliated structures. Additionally, exfoliated structures only occur when very favorable surface−polymer interactions exist.

5. Conclusions

The mean-field statistical lattice model developed serves as a first approximation to the polymer melt intercalation process. It may be used to address thermodynamic issues associated with hybrid formation and identify possible equilibrium states of the hybrids. In general, an interplay of entropic and energetic factors determines the outcome of polymer intercalation. The model indicates that the entropic penalty of polymer confinement may be compensated for, for gallery heights up to the length of the fully-extended tethered chains, by the increased conformational freedom of the tethered chains as the layers separate. When the total entropy change is small, small changes in the system's internal energy will determine if intercalation is thermodynamically possible. Complete layer separation, though, depends on the establishment of very favorable polymer−OLS interactions to overcome the penalty of polymer confinement. For alkylammonium-modified layered silicates, a favorable energy change is accentuated by maximizing the magnitude and number of favorable polymer−surface interactions while minimizing the magnitude and number of unfavorable apolar interactions between the polymer and the tethered surfactant chains. If complete layer separation is achieved ($h > R_0$), the total entropy change is near zero again, and the potential stability of the hybrid may be thought of in terms of a blend of two macromolecules. The model's free energy curves and their dependence on energetic and entropic factors suggest three possible equilibrium states—immiscible, intercalated, and exfoliated—all of which have been experimentally observed.

The model has been successful in addressing some thermodynamic issues associated with hybrid formation. However, the mean-field approach and its assumptions somewhat limit the usefulness of the model in quantitatively predicting the results of melt intercalation reactions and describing situations where the OLS's interlayer is not completely occupied by tethered-chain segments, which is the case for many silicates having low charge densities or modified by short surfactant chains. Some of the limitations and gross approximations of the model, such as the decoupling of the tethered chain and polymer conformations in the interlayer, may be addressed by developing more sophisticated models of hybrid formation based on the theories of Scheutjens and Fleer[37] and Szleifer.[43] However, the lack of experimentally determined molecular interactions still restricts the qualitative usefulness of these more sophisticated approaches. Therefore, to improve our understanding of the microscopic environment of the interlayer, Monte-Carlo and molecular dynamic simulations of hybrid formation and of intercalation of small molecules in layered materials are being conducted to provide additional insights into the mechanisms and important factors associated with intercalation. Recent Monte-Carlo simulations of the absorption of short chains in a slit exhibit equilibrium structures very similar to those concluded by our model.[64]

The present model, although simplified to obtain solutions in closed form, provides some general and physically sound directives for the development of polymer−OLS nanocomposites via polymer melt intercalation. Using the model and experimental results, a followup paper will consider the effect of intermolecular interactions and silicate functionalization on hybrid formation and propose guidelines for the selection of potentially successful OLS−polymer combinations.[28]

Acknowledgment. This work was supported by NSF (DMR-9424446) and by generous gifts from DuPont, Exxon, Hercules, Monsanto, Nanocor, Southern Clay Products, and Xerox. R.A.V. gratefully acknowledges the partial support of a NDSEG Fellowship. We would like to thank E. J. Kramer, T. Panagiotopoulos, J. Marko, I. Szleifer, L. Vega, and R. Krishnamoorti and the anonymous reviewers of the manuscript for constructive comments. This study benefited from the use of Material Science Central Facilities at Cornell.

Index of Symbols

1	confined polymer
2	tethered surfactant chains
a_i	segment length (i = l or 2)
a_p	statistical segment length of the polymer
c	statistical surface factor
h	gallery height
h_0	initial gallery height
h_c	gallery height where $\Delta s_V \sim 0$
h_∞	extended length of the tethered chain
k_B	Boltzmann's constant
m_i	number of segments in the chain (i = 1 or 2)
n'	number of carbon atoms in the alkyl chain
n_0	total number of lattice sites
u	dimensionless excluded volume parameter[34]
v_i	molar volume per segment (i = l or 2)
A	number of lattice sites in contact with a surface
A_{jk}^i	total area of contact between the components for the initial unintercalated system
A_{jk}^f	total area of contact between the components for the final hybrid
N_A	Avogadro's number
α	polymer chain expansivity[49]
α_i	interaction area per segment (i = 1 or 2)
ϵ_{jk}	pairwise interaction energy per area of j−k contacts relative to j−j and k−k contacts
η_{i+1}	number of conformations available to the ith + 1 tethered chain
ξ_c	critical interlayer structure parameter
σ	area per tethered chain
$\hat{\varphi}_i$	interlayer volume fraction (i = 1 or 2)
χ_s	fraction of interlayer volume next to the surface accessible by the tethered chains at h
χ_{S0}	fraction of interlayer volume next to the surface accessible by the tethered chains at h_0

References and Notes

(1) Brus, L. E.; Brown, W. L.; Andres, R. P.; Averback, R. S.; Goddard, W. A., III; Kaldor, A.; Louie, S. G.; Moskovits, M.; Peercy, P. S.; Riley, S. J.; Siegel, R. W.; Spacpen, F.A.; Wang, *Y. J. Mater. Res.* **1989**, *4*, 704.
(2) Research Opportunities for Materials with Ultrafine Microstructures; National Research Council, National Academy Press: Alexandria, VA, 1989.
(3) *Science* **1991**, *254*, l300.
(4) Vaia, R. A.; Ishii, H.; Giannelis, E. G. *Chem. Mater.* **1993**, *5*, 1694.
(5) Vaia, R. A.; Vasudevan, S.; Krawiec, W.; Scanlon, L. G.; Giannelis, E. P. *Adv. Mater.* **1995**, *7*, 154.
(6) Vaia, R. A.; Jandt, K. D.; Kramer, E. J.; Giannelis, E. P. *Macromolecules* **1995**, *28*, 8086.
(7) Vaia, R. A. Doctoral Thesis, Cornell University, 1995.
(8) Cao, G.; Mallouk, T. E. J. *Solid State Chem.* **1991**, *94*, 59.
(9) Pillion, J. E.; Thompson, M. E. *Chem. Mater.* **1991**, *3*, 777.
(10) l0. Kanatzidis, M. G.; Wu, C.-G.; Marcy, H. O.; DeGroot, D. C.; Kannewurf, C. R. *Chem. Mater.* **1990**, *2*, 222.
(11) ll. Liu, Y. J.; DeGroot, D. C.; Schindler, J. L.; Kannewurf, C. R.; Kanatzidis, M. G. *Chem. Mater.* **1991**, *3*, 992.

(12) Kanatzidis, M. G.; Wu, C.-G.; DeGroot, D. C.; Schindler, J. L.; Benz, M.; LeGoff, E.; Kannewurf, C. R. In *NATO ASI. Chemical Physics of Intercalation II;* Fisher, J., Ed.; Plenum Press: New York, 1993.
(13) Kato, C.; Kuroda, K.; Takahara, H. *Clays Clay Miner.* **1981**, *29*, 294.
(14) Ogawa, M.; Kuroda, K.; Kato, C. *Clay Sci.* **1989**, *7*, 243.
(15) Fukushima, Y.; Okada, A.; Kawasumi, M.; Kurauchi, T.; Kamigaito, O. *Clay Miner.* **1988**, *23*, 27.
(16) Usuki, A.; et al. J. *Mater. Res.* **1993**, *8*, 1179.
(17) Wang, M. S.; Pinnavaia, T. J. *Chem. Mater.* **1994**, *6*, 2216.
(18) Mehrotra, V.; Giannelis, E. P. In *Polymer Based Molecular Composites;* Shaefer, D. W., Mark, J. E., Eds.; MRS Proceedings: Pittsburgh, PA, 1990; p 171.
(19) Mehrotra, V.; Giannelis, E. P. *Solid State Commun.* **1991**, *77*, 155.
(20) Mehrotra, V.; Giannelis, E. P. *Solid State Ionics* **1992**, *51*, 115.
(21) Messersmith, P.; Giannelis, E. P. *Chem. Mater.* **1994**, *6*, 1719.
(22) Messersmith, P.; Giannelis, E. P. *J. Polym. Sci. Part A: Polym. Chem.* **1995**, *33*, 1047.
(23) Giannelis, E. P.; Mehrotra, V.; Tse, O. K.; Vaia, R. A.; Sung, T.-C. In *Synthesis and Processing of Ceramics: Scientific Issues;* Rhine, W. E., Shaw, T. M., Gottshall, R. J., Chen, Y., Eds.; MRS Proceedings: Pittsburgh, PA, 1992; pp 249, 547.
(24) Aranda, P.; Ruiz-Hitzky, E. *Chem. Mater.* **1992**, *4*, 1395.
(25) Messersmith, P. B.; Stupp, S. I. J. *Mater. Res.* **1992**, *7*, 2599.
(26) Nazar, L. F.; et al. *Solid State Ionics II;* MRS Proceedings: Pittsburgh, PA, 1991; p 210.
(27) Yano, K.; et al. *J. Polym. Sci., Part A: Polym. Chem.* **1993**, *31*, 2493.
(28) Vaia, R. A; Giannelis, E. P. *Macromolecules* **1997**, 30, 8000.
(29) Pinnavaia, T. J. *Science* **1983**, *220*, 365.
(30) Brindley, S. W., Brown, G., Eds. *Crystal Structure of Clay Minerals and their X-ray Diffraction;* Mineralogical Society: London, 1980.
(31) Vaia, R. A.; Teukolsky, R. K.; Giannelis, E. P. *Chem. Mater.* **1994**, *6*, 1017.
(32) de Gennes, P. G. *Scaling Concepts in Polymer Physics;* Cornell University Press: Ithaca, NY, 1979 (see also references therein).
(33) Hesselink, F. T. *J. Phys. Chem.* **1969**, *73*, 3488.
(34) Dolan, A. K.; Edwards, S. F. *Proc. R. Soc. London, Ser. A* **1975**, *343*, 427.
(35) Gerber, P. R.; Moore, M. A. *Macromolecules* **1977**, *10*, 476.
(36) Levine, S.; Thomlinson, M. M.; Robinson, K. *Faraday Discuss. Chem. Soc.*, **1978**, *65*, 202.
(37) Scheutjens, J. M. H. M.; Fleer, G. J. *J. Phys. Chem.* **1979**, *83*, 1619.
(38) Scheutjens, J. M. H. M.; Fleer, G. J. *Macromolecules* **1985**, *18*, 1882.
(39) Ligoure, C.; Leibler, L. J. *Phys. Fr.* **1990**, *51*, 1313.
(40) Carignano, M. A.; Szleifer, I. J. *Chem. Phys.* **1994**, *210*, 3100.
(41) Mackor, E. L.; van der Waals, J. H. *J. Colloid Sci.* **1952**, *7*, 535.
(42) Dill, K. A.; Cantor, R. S. *Macromolecules* **1984**, *17*, 380.
(43) Szleifer, I.; Ben-Shaul, A.; Gelbart, W. M. *J. Chem. Phys.* **1986**, *85*, 5345.
(44) Szleifer, I.; Ben-Shaul, A.; Gelbart, W. M. *J. Phys. Chem.* **1990**, *94*, 5081.
(45) Helfand, E. *Macromolecules* **1975**, *8*, 552.
(46) Whitmore, M. D.; Noolandi, J. *Macromolecules* **1985**, *18*, 2486.
(47) Evers, O. A.; Scheutjens, J. M. H. M.; Fleer, G. J. *Macromolecules* **1990**, *23*, 5221.
(48) Shull, K. R.; Winey, K. I. *Macromolecules* **1992**, *25*, 2637-2644.
(49) Flory, P. J. *Principles of Polymer Chemistry;* Cornell University Press: Ithaca, NY, 1953.
(50) Barrer, R. M.; Kelsly, K. E. *Faraday Soc. Trans.* **1961**, *57*, 625.
(51) Klatte, S. J.; Beck, T. L. *J. Phys. Chem.* **1993**, *97*, 5727. Vacatello, M.; Yoon, D. Y.; Laskowski, B. C. *J. Chem. Phys.* **1990**, *93*, 779.
(52) There are several expressions in the literature for polymer brushes that can be derived by assuming the tethered chains occupy a cylinder, hemisphere, or combinations thereof with a diameter related to the packing density of the chains and thus the initial gallery height, h_0. However, these alternative expressions do not add any additional qualitative insight to that obtained from the random-flight approximation.
(53) de Gennes, P. G. *Macromolecules* **l980**, *13*, 1069.
(54) Wittkop, M.; Kreitmeier, S.; Goritz, D. *Macromolecules* **1996**, *29*, 4754.
(55) For simplicity, the ammonium head group of the aliphatic chains is assumed to interact with the system as part of the silicate surface.
(56) van Oss, C. J. *Interfacial Forces in Aqueous Media;* Marcel Decker: New York, 1994.
(57) Konigsveld, R.; Kleintjens, L. A. *Macromolecules* **1971**, *4*, 637.
(58) van Opstal, L.; Konigsveld, R.; Kleintjens, L. A. *Macromolecules* **1991**, *24*, 161.
(59) The effective interaction parameter is commonly expressed as $a + b/Q$, where a is an empirical entropy correction factor that has been found to be necessary for qualitative agreement with experiment.[58] For our purpose of establishing trends and guidelines, a is assumed to be zero.
(60) Theng, B. K. G. *Formation and Properties of Clay-Polymer Complexes;* Elsevier: New York, 1979.
(61) The length of a fully-extended alkylammonium chain may also be approximated as $(n' - 1)0.127 + A + B$ nm where n' is the number of carbon atoms and A and B are the size of an ammonium and a methyl group.[30] Although this expression improves the approximation of the extended chain length by 5−10%, it substantially increases the complexity of the theoretical expressions because of the increased number of different segment units used to describe the tethered chain.
(62) Olabisi, O.; Robenson, L. M.; Shaw, M. T. *Polymer-Polymer Miscibility;* Academic: New York, 1979.
(63) Burnside, S. D.; Giannelis, E. P. *Chem. Mater.* **1995**, *7*, 1597.
(64) Vega, L. F.; Panagiotopoulos, A. Z.; Gubbins, K. E. *Chem. Eng. Sci.* **1994,** *49*, 2921.

MA9514333